

Evaluating potential impacts of a preferential vaccine recommendation for adults aged 65 and older on United States influenza burden

eAppendix

Supplementary text

Mathematical model

The model consists of a system of ordinary differential equations (ODEs) describing the infection and progression of influenza within a well-mixed population. Let S denote susceptible individuals, E exposed, A asymptomatic (or presymptomatic) and infectious, I infectious and potentially symptomatic, and R recovered and immune. Then for age group a , the unvaccinated population is modeled as

$$\begin{aligned}\frac{dS_a}{dt} &= -\lambda_a S_a - v_a^S S_a - v_a^H S_a \\ \frac{dE_a}{dt} &= \lambda_a S_a - \sigma E_a \\ \frac{dA_a}{dt} &= \sigma E_a - \gamma_1 A_a \\ \frac{dI_a}{dt} &= \gamma_1 A_a - \gamma_2 I_a \\ \frac{dR_a}{dt} &= \gamma_2 I_a,\end{aligned}$$

where λ_a is the force of infection experienced by age group a (details below); $1/\sigma$ is the incubation period; and $1/\gamma_1 + 1/\gamma_2$ is the infectious period. We do not include births, deaths from causes other than influenza, or aging in this model as we are only considering short-term dynamics from a single season. We assume a fraction of infectious individuals, f_a , will develop symptoms, so that the total symptomatic in age group a is $f_a I_a$. For these individuals, $1/\gamma_1$ and $1/\gamma_2$ are the pre-symptomatic and symptomatic infectious periods, respectively. Finally, v_a^S and v_a^H are the rates of vaccination with standard vaccines (SVs) and higher-dose and adjuvanted vaccines (HDAVs) in age group a , respectively. Note that $v_a^H = 0$ for all age groups except the over 65s.

To model the vaccinated population we use the superscript $X = S, H$ to denote vaccination with an

SV or HDAV, respectively. The corresponding equations can then be expressed as

$$\begin{aligned}
\frac{dS_a^X}{dt} &= v_a^X S_a^X - (1 - VEi_a^X) \lambda_a S_a^X \\
\frac{dE_a^X}{dt} &= (1 - VEi_a^X) \lambda_a S_a^X - \sigma E_a^X \\
\frac{dA_a^X}{dt} &= \sigma E_a^X - \gamma_1 A_a^X \\
\frac{dI_a^X}{dt} &= \gamma_1 A_a^X - \gamma_2 I_a^X \\
\frac{dR_a^X}{dt} &= \gamma_2 I_a^X,
\end{aligned}$$

where VEi_a^X is the effectiveness of vaccine X against infection in age group a . The total symptomatic is $f_a(1 - VE s_a^X) I_a^X$, where $VE s_a^X$ is the effectiveness of vaccine X (SV or HDAV) against developing symptoms in age group a .

Force of infection Let \bar{C} denote the synthetic contact matrix (eFigure 2), so that $C_{i,j}$ is the average number of daily contacts experienced by someone in age group a from someone in age group j . The force of infection is defined as

$$\lambda_a = \frac{\beta}{N_a} \sum_{j=1}^6 C_{a,j} (A_j + I_j + (1 - VE t_j^S)(A_j^S + I_j^S) + (1 - VE t_j^H)(A_j^H + I_j^H))$$

where N_a is the population size of age group a , β is the probability of transmission given contact with an infectious individual, and $VE t_a^X$ is the effectiveness of vaccine X against onward transmission in age group a . We calculated β from the R_0 values given in eTable 1 using the next generation matrix relationship that R_0 is the dominant eigenvalue of $\frac{\beta}{(\gamma_1 + \gamma_2)} \bar{C}$, and γ_1, γ_2 , and \bar{C} are all known inputs.

Contact patterns The age-specific contact matrix \bar{C} was generated using a synthetic contact matrix developed for the US (eFigure 2) (1–3). The original matrix included all contact settings (home, work, school, and other locations) and entries were reported in 5 year age bands (0–4, 5–9, etc). We aggregated the entries of this matrix to match the six age groups of our model using the `flumodels` package. Since our analysis did not consider non-pharmaceutical interventions such as physical distancing, we assumed \bar{C} was fixed for the duration of each simulation.

Influenza burden Finally, we track the burden of influenza through individuals who experience symptoms, F_a , who are hospitalized, H_a , and who die, D_a . The equations are given by

$$\begin{aligned}\frac{dF_a}{dt} &= f_a \gamma_1 (A_a + A_a^S (1 - VE_s^S) + A_a^H (1 - VE_s^H)) - dF_a \\ \frac{dH_a}{dt} &= dc_a F_a - sH_a \\ \frac{dD_a}{dt} &= sh_a H_a,\end{aligned}$$

where $1/d$ is the average delay from developing symptoms to hospital admittance or symptom resolution; c_a is the case-hospitalization ratio (CHR) for age group a ; h_a is the corresponding hospitalization-fatality ratio (HFR); and $1/s$ is the average length of stay in hospital.

Calibrating the baseline model

We verified that symptomatic cases peaked within the range of previous seasons (eFigure 5A) and accumulated at a slower rate than vaccination coverage, consistent with trends typically observed during U.S. influenza seasons (eFigure 5B) (4, 5). The model also captured the observed age distribution of symptomatic cases, which occur mostly in the 5–17 and 18–49 age groups, and hospitalizations and deaths, which occur mostly in adults ≥ 65 (eFigure 5C–E). Finally, the total number of simulated symptomatic cases, hospitalizations and deaths were within reported ranges from previous moderate-/high- and moderate-/low-severity seasons (eTable 3). Incorporating uncertainty in the proportion of vaccinees ≥ 65 receiving a HDAV at baseline, and relative effectiveness of HDAVs compared to SVs (rVE) did not impact these conclusions (eFigures 6 and 7).

Supplementary tables

eTable 1 – Parameter values for baseline and trade-off scenarios. R_0 = basic reproduction number; R_e = effective reproduction number = R_0 (1 - initial proportion immune); VE = vaccine effectiveness; SV = standard vaccine; HDAV = higher-dose and adjuvanted vaccine.

Parameter	Additional description	Season severity	Initial value	Range*	References
Epidemiological					
Latent period	Time from infection to onset of infectiousness		1 day		(6–8)
Pre-symptomatic infectious period	Time from onset of infectiousness to onset of symptoms		1 day		(7, 9)
Symptomatic infectious period			2 days		(7, 10)
Asymptomatic infectious period			3 days		(7, 9, 10)
Symptomatic fraction, $\geq 65^{**}$	Fraction of infections that are symptomatic		0.55		(7, 11–13)
Relative infectivity of asymptomatic infections			1		(9)
Initial proportion immune	Proportion of individuals with pre-existing immunity		0.15		***
R_0 (R_e)		High Low	1.4 (1.2) 1.3 (1.1)		(14)***
Peak transmission	Day when seasonality in transmission peaks	High Low	120 160		***

eTable 1 continued

Parameter	Additional description	Season severity	Initial value	Range*	References
CHR, $\geq 65^{**}$	Ratio of hospitalizations to symptomatic cases		0.09		(15)
HFR, $\geq 65^{**}$	Ratio of deaths to hospitalizations		0.12		(15)
Vaccination					
Standard VE against symptoms	Average effectiveness of SVs, all ages	High Low	0.35 0.5		(16)
Standard VE against symptoms, ≥ 65	Average effectiveness of SVs, ≥ 65	High Low	0.25 0.4		(16)
Relative VE, $\geq 65^\dagger$	Relative effectiveness of HDAVs compared to SVs, ≥ 65		15%	5–35%	(17)
VE against infection			0	0 or 10% of VE against symptoms	
VE against onward transmission			0	0 or 10% of VE against symptoms	
Initial HDAV uptake	Proportion of vaccinees ≥ 65 who receive a HDAV at baseline		0.75	0.6–0.8	(18–20)
Benefits					

eTable 1 continued

Parameter	Additional description	Season severity	Initial value	Range*	References
Increase in HDAV uptake	Proportion of vaccinees ≥ 65 who switch from SV to HDAV		N/A	0–0.2 above initial HDAV uptake	
Tradeoffs					
Delay in additional HDAV uptake	Delay in additional HDAV coverage among the proportion who switch from SV to HDAV		N/A	0, 3, 6 weeks (discrete) 0–6 weeks (continuous)	
Reduction in overall coverage	Proportion of vaccinees offered SVs who decide to forego vaccination		N/A	0, 0.1, 0.2 (discrete) 0–0.2 (continuous)	

*If included in sensitivity analyses; ** values used for other age groups are listed in eTable 2; ***calibrated values.

†Relative VE values correspond to an absolute HDAV VE of 0.36 (0.29–0.51) in the high-severity season and

0.49 (0.43–0.61) in the low-severity season.

eTable 2 – Parameter values that vary by age. VE = vaccine effectiveness.

Parameter	Age	Season severity	Value	References
Symptomatic fraction	0–4		0.80	(13)
	5–12		0.50	
	13–17		0.60	
	18–49		0.40	
	50–64		0.50	
	≥65		0.55	
Case-hospitalization ratio ($\times 10^{-3}$)	0–4		6.97	(15)
	5–12*		2.74	
	13–17*		2.74	
	18–49		5.61	
	50–64		10.6	
	≥65		90.9	
Hospitalization-fatality ratio ($\times 10^{-3}$)	0–4		9.70	(15)
	5–12*		17.2	
	13–17*		17.2	
	18–49		31.0	
	50–64		53.9	
	≥65		116	
Standard vaccine VE against symptoms	0–4	High	0.45	(16)
	5–12	High	0.40	
	13–17	High	0.35	
	18–49	High	0.30	
	50–64	High	0.35	
	≥65	High	0.25	
	0–4	Low	0.60	
	5–12	Low	0.55	
	13–17	Low	0.50	
	18–49	Low	0.45	
	50–64	Low	0.50	
	≥65	Low	0.40	

*5–12 and 13–17 were assigned the same values to match the resolution of the data (5–17).

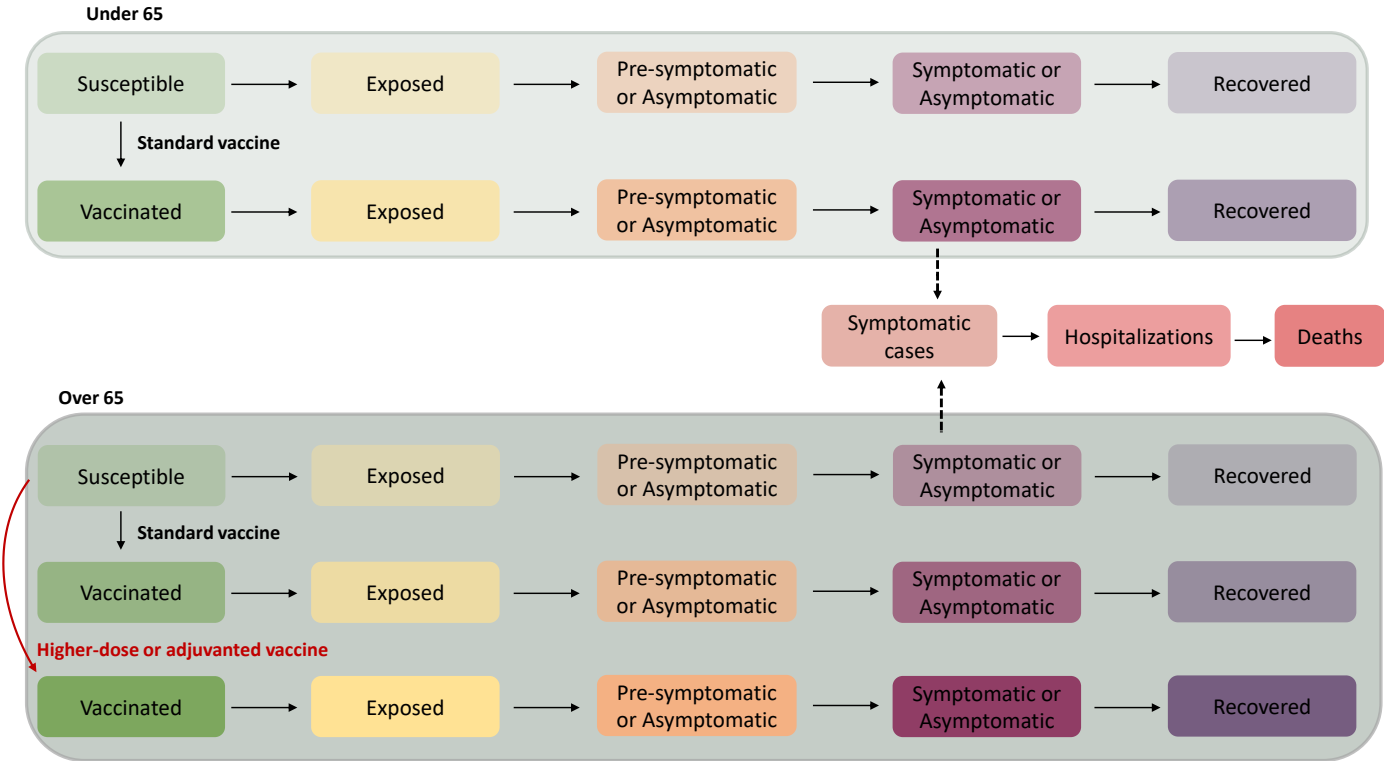
eTable 3 – Total burden output from the baseline simulations compared to reports from the 2011/12-2018/19 seasons.

Burden metric*	Season severity	Model simulation	Reported range [†]
Cases	High/moderate	41.3 million	29–41 million
Cases	Low/moderate	17.5 million	9–29 million
Hospitalizations	High/moderate	536,000	350,000–710,000
Hospitalizations	Low/moderate	207,000	140,000–380,000
Deaths	High/moderate	45,000	38,000–52,000
Deaths	Low/moderate	17,000	12,000–28,000

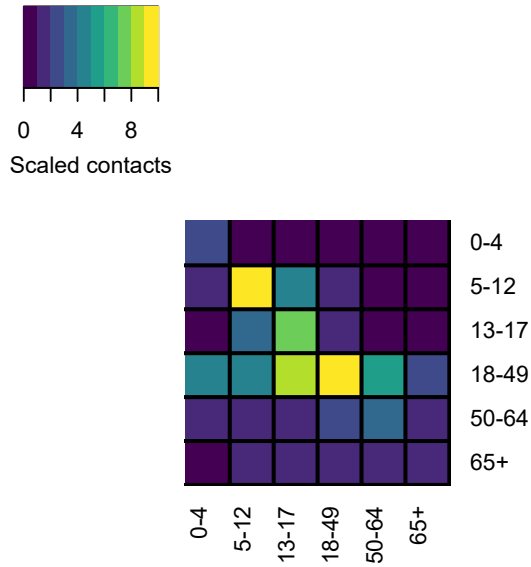
* Hospitalizations are based on laboratory-confirmed influenza-associated hospitalizations; cases and deaths are calculated from these using estimates of how many cases and deaths occur for each hospitalization. See www.cdc.gov/flu/about/burden for further details (15).

[†]Ranges for the high-/moderate-severity season incorporate reports from 2012/13, 2013/14, 2014/15, 2016/17 and 2017/18; ranges for the low-/moderate-severity season incorporate reports from 2011/12, 2015/16 and 2018/19.

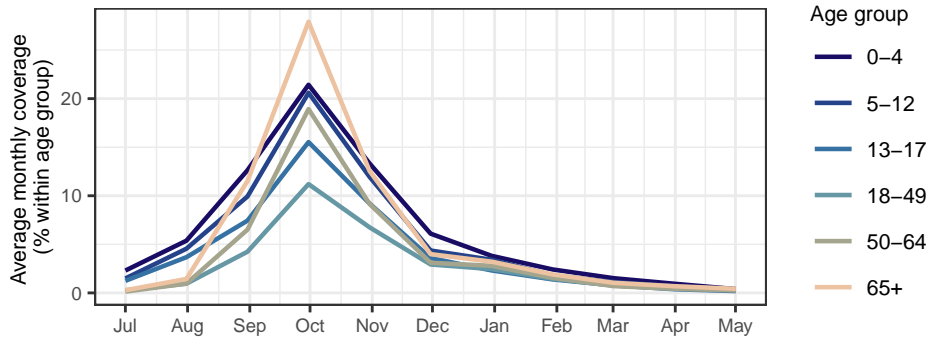
Supplementary figures



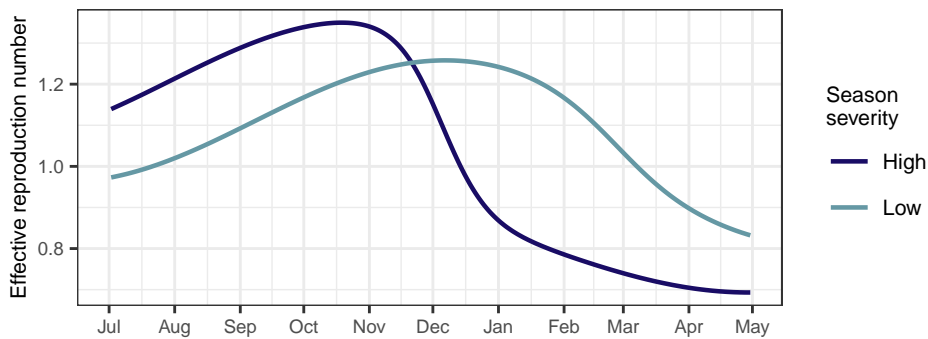
eFigure 1 – Model schematic. Equations are given in the supplementary text above.



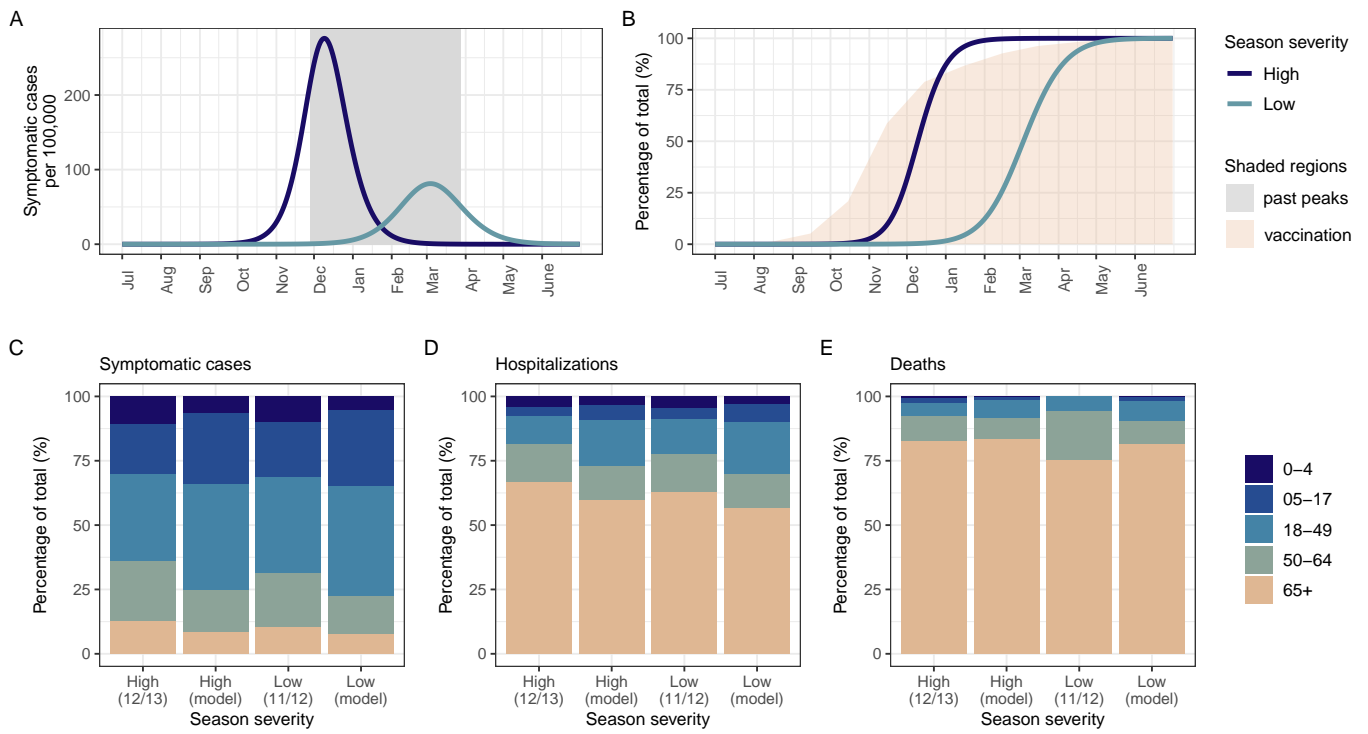
eFigure 2 – Age-specific contact patterns. Contact patterns between the six age groups defined in our analysis were inferred from a synthetic contact matrix designed for the United States (3).



eFigure 3 – Average monthly vaccine coverage within each age group. Data were obtained from FluVaxView from the 2011/12–2018/19 influenza seasons (4) and include all vaccine types (i.e. SV and HDAV).

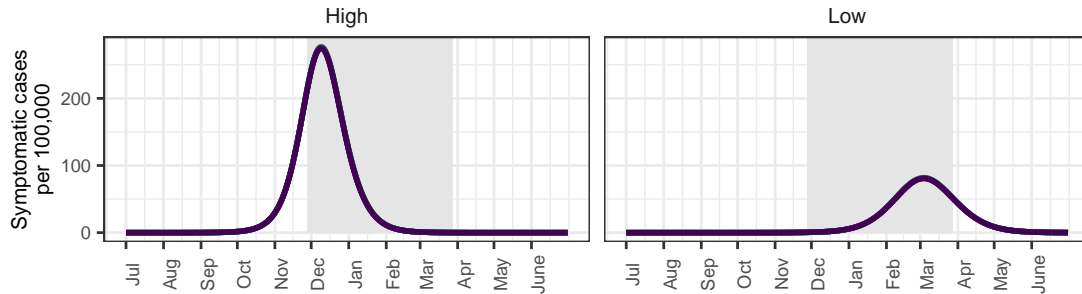
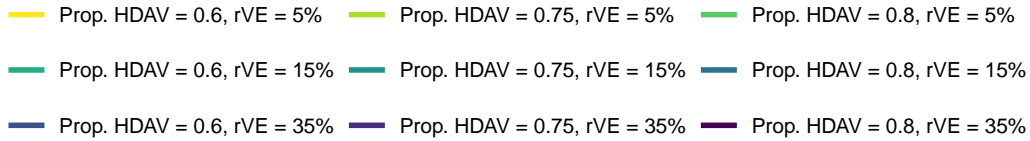


eFigure 4 – Seasonality in transmission. The effective reproduction number (R_e) was calculated as $R_0 \times (1 - \text{the proportion immune})$. Parameters were calibrated to generate epidemic dynamics in line with previous seasons (see eTable 1 for values).

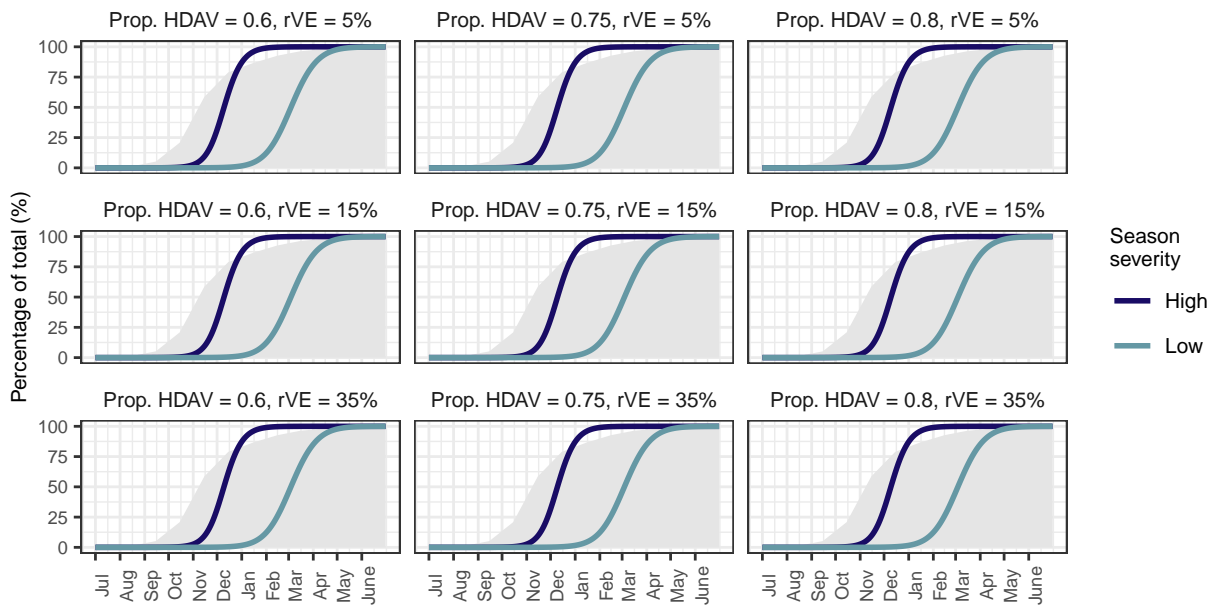


eFigure 5 – The baseline model generates epidemic dynamics consistent with previous seasons. (A) Solid lines represent the incidence of symptomatic infections (per 100,000 people) in each season (high or low severity) and for all age groups. The grey shaded region indicates when the 2011/12–2018/19 seasons peaked. (B) Solid lines show cumulative symptomatic cases as a percentage of the final total, and the light shaded region indicates cumulative vaccinations as a percentage of final coverage. (C-F) Age distributions of symptomatic cases (C), hospitalizations (D) and deaths (E) from the two baseline model seasons (labeled 'High' and 'Low') compared to representative data from 2012/13 (a high-/moderate-severity season) and 2011/12 (a low-severity season). The 5–12 and 13–17 age groups from the model output were combined to match the format of the aggregated data (5–17).

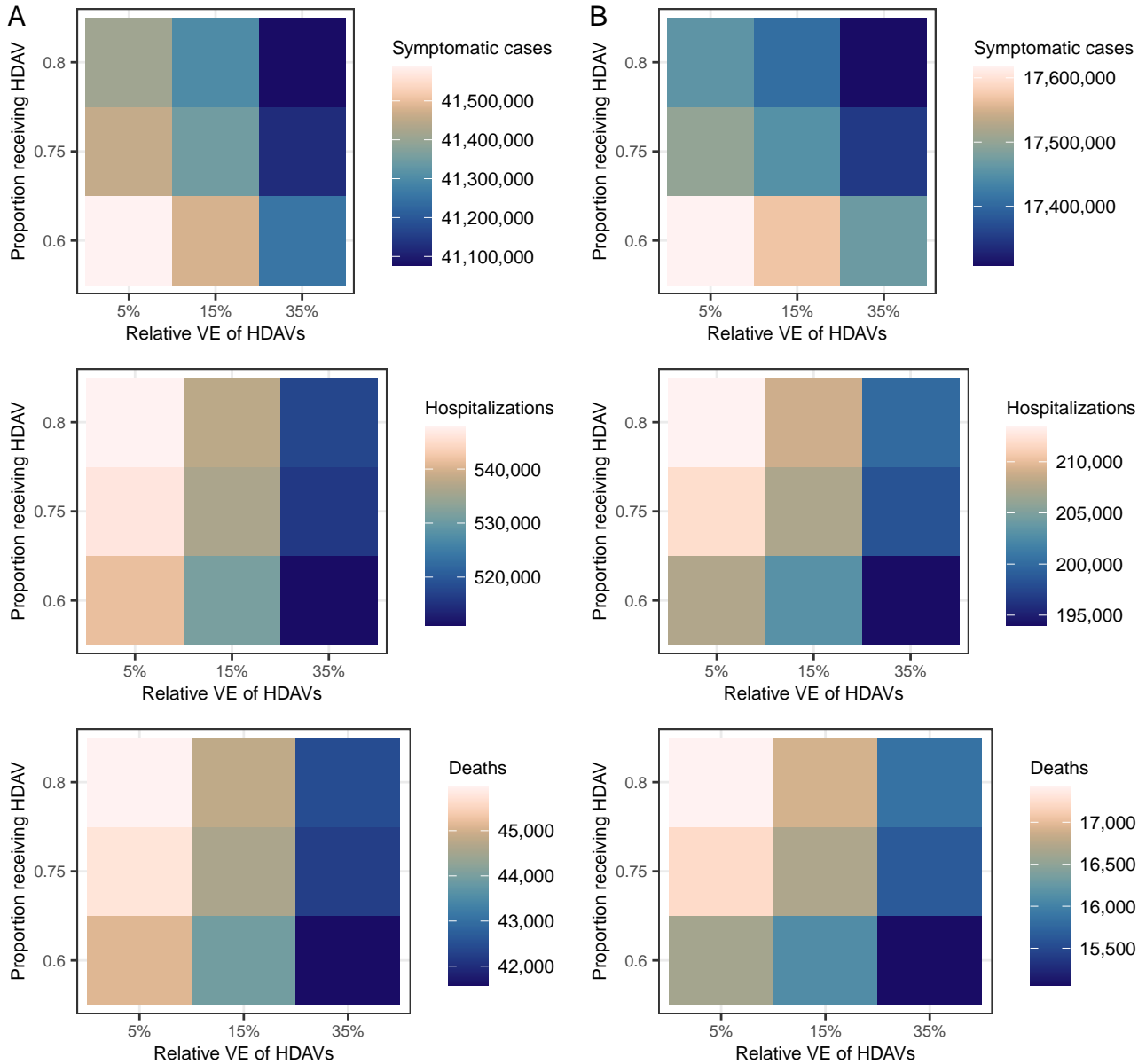
A



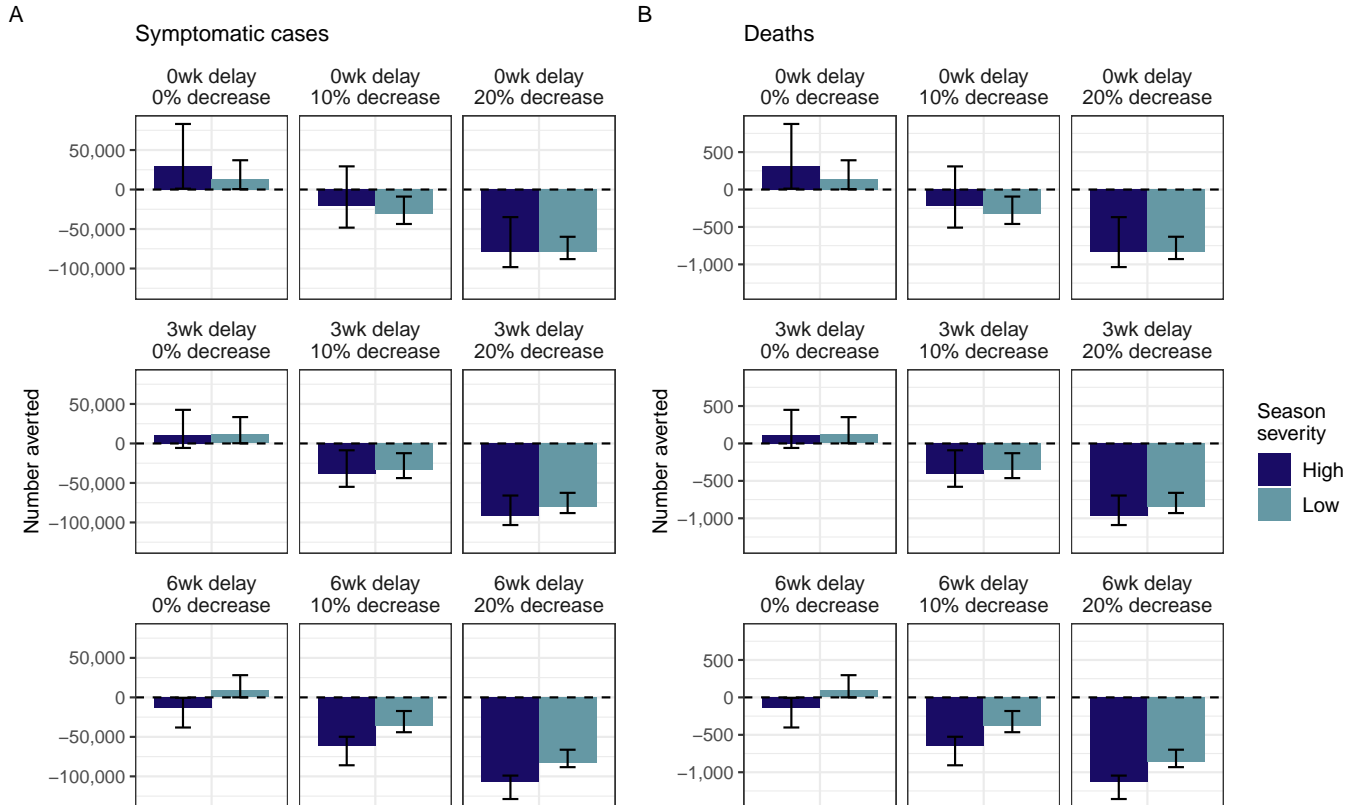
B



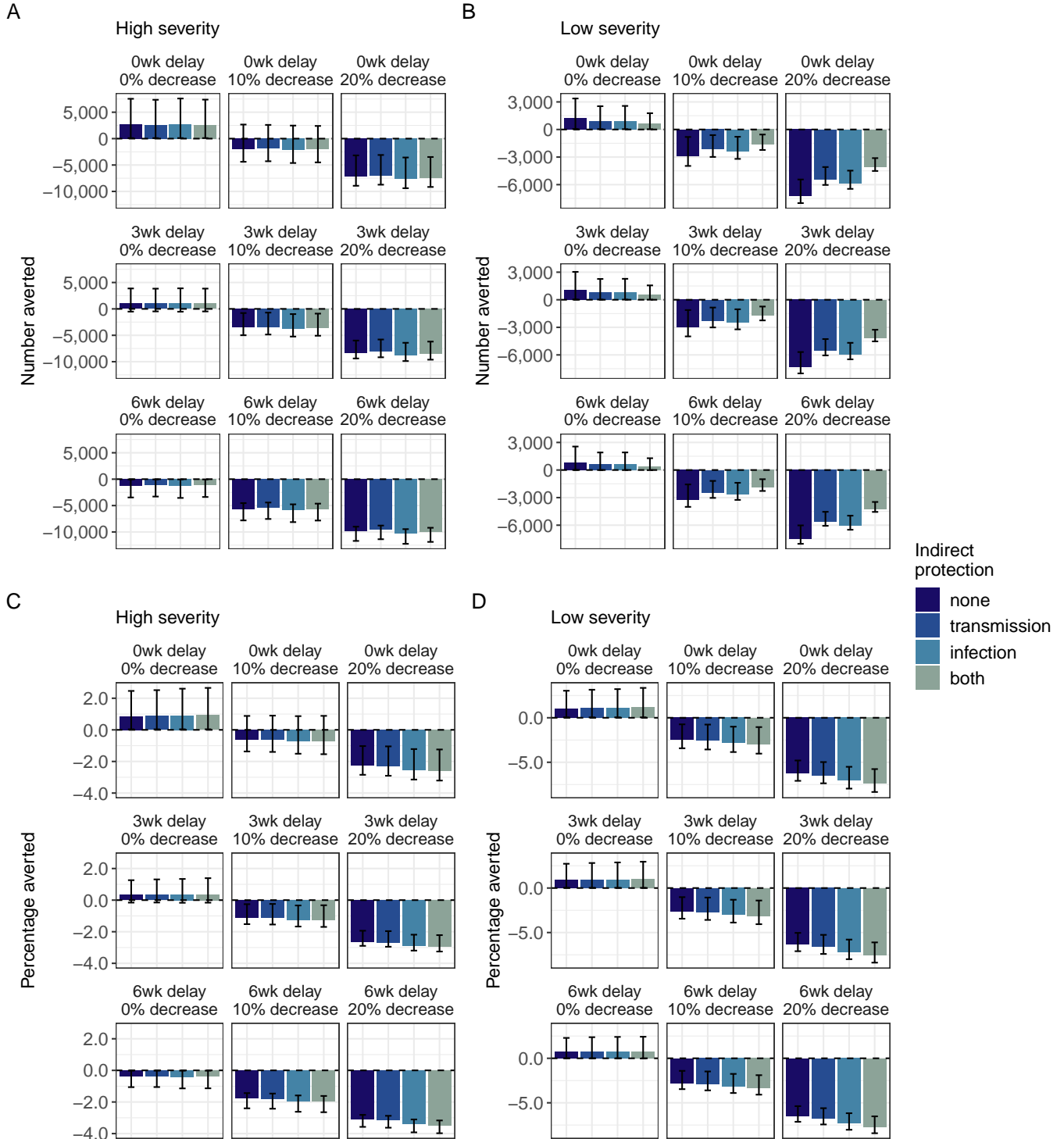
eFigure 6 – The baseline model still captures epidemic dynamics observed in previous seasons when HDAV parameter uncertainty is incorporated. The proportion of over 65 vaccinees receiving a HDAV ('Prop. HDAV') takes the values 0.6 (lower bound of uncertainty range), 0.75 (original value in Figure 1) and 0.8 (upper bound); the relative effectiveness of HDAVs compared to SVs (rVE) takes the values 5% (lower bound), 15% (original value) and 35% (upper bound). (A) Solid lines represent the incidence of symptomatic infections (per 100,000 people) for each combination of HDAV parameters. The grey shaded region indicates when the 2011/12–2018/19 seasons peaked, and the panels distinguish between the high severity (left) and low severity (right) seasons. (B) Solid lines show cumulative symptomatic cases as a percentage of the final total, and the grey shaded region indicates cumulative vaccinations as a percentage of final coverage. Each panel is a different combination of HDAV parameters.



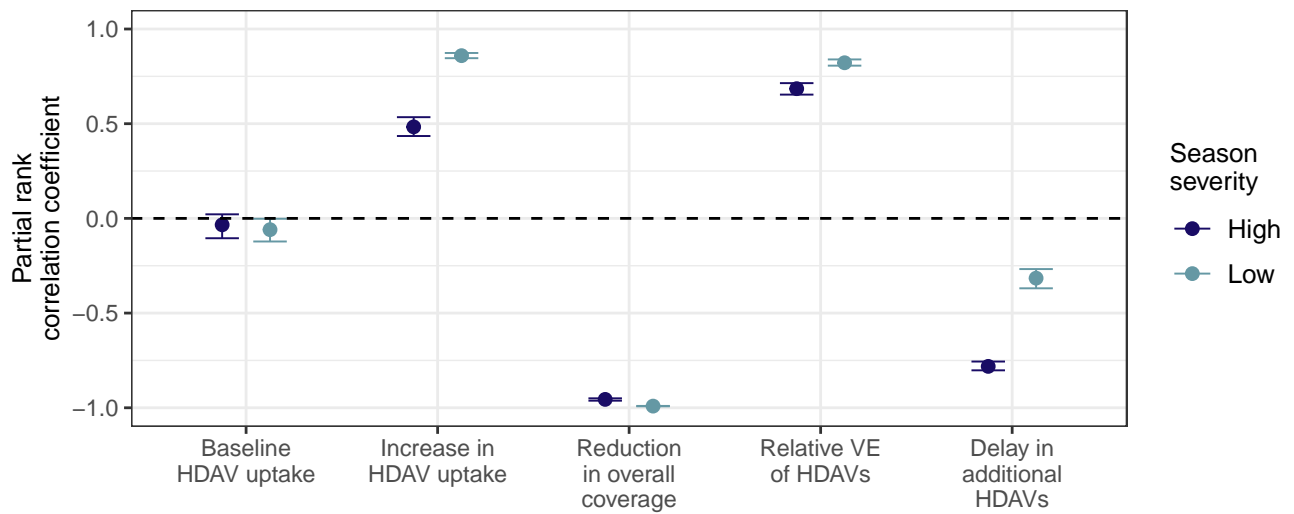
eFigure 7 – Total burden predicted by the baseline model is still within range of previous seasons when HDAV parameter uncertainty is incorporated. The proportion of vaccinees ≥ 65 receiving a HDAV takes the values 0.6 (lower bound of uncertainty range), 0.75 (original value in Figure 1) and 0.8 (upper bound); the relative effectiveness of HDAVs compared to SVs takes the values 5% (lower bound), 15% (original value) and 35% (upper bound). Panels show the total number of symptomatic cases, hospitalizations, or deaths for the high severity (A) and low severity (B) seasons and each combination of HDAV parameters.



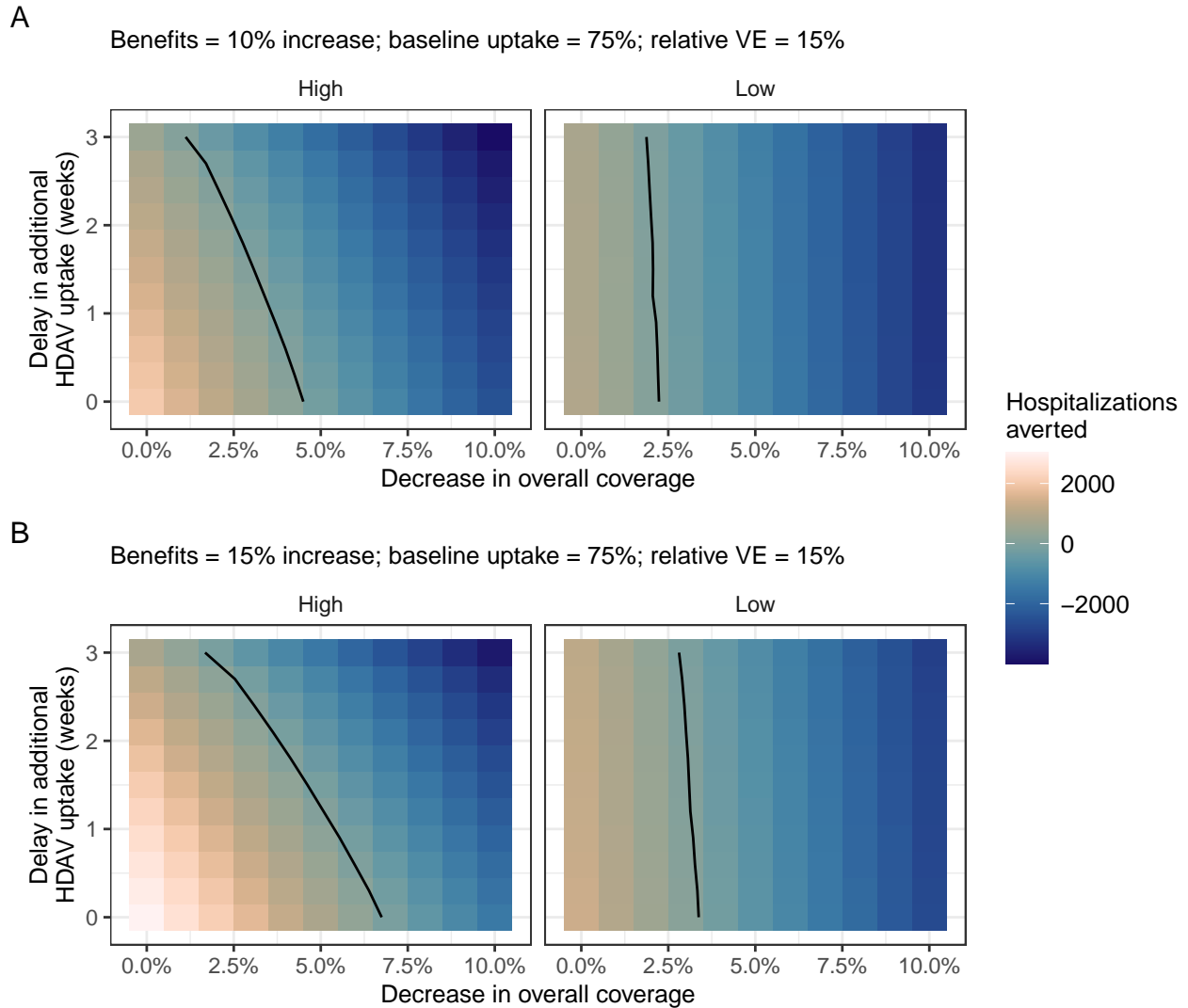
eFigure 8 – Averted burden in adults ≥ 65 under different tradeoff scenarios. Bars indicate the mean number of averted symptomatic cases (A) and deaths (B) from 1000 different Latin hypercube parameter combinations; error bars are the 95th percentiles. Each panel shows a different combination of the delay in administration of additional HDAVs (0, 3, or 6 weeks), and reduction in overall vaccine coverage (0, 10, or 20%). Positive values indicate a decrease in burden relative to the corresponding baseline simulation and therefore a positive impact of the new recommendation.



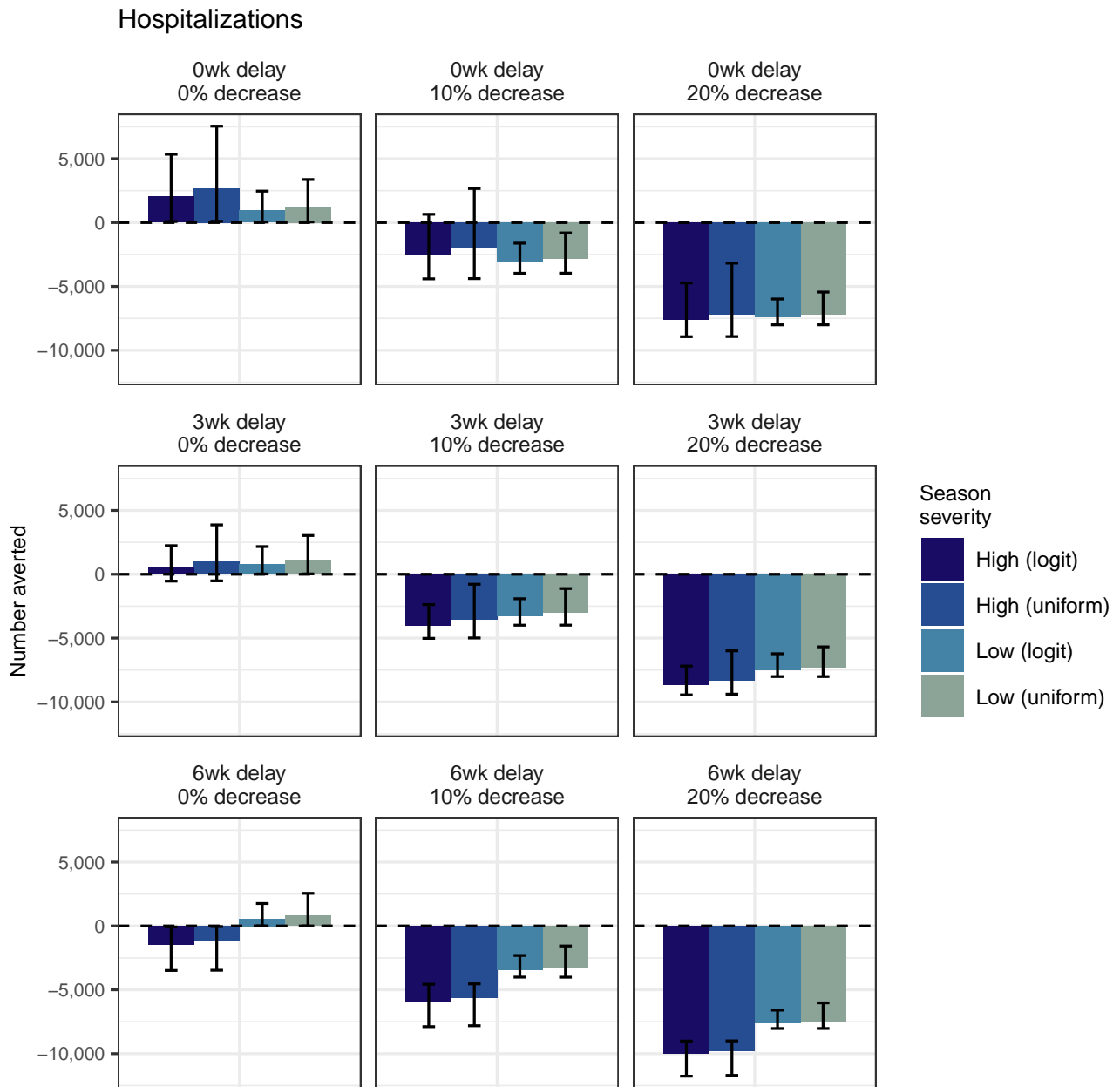
eFigure 9 – Burden averted when vaccine effectiveness (SV and HDAV) against infection and transmission is 10% of vaccine effectiveness against symptoms. Indirect protection occurs through a non-zero vaccine effectiveness against infection or transmission or both. No indirect protection occurs when vaccines only protect against symptoms (i.e. Fig 1 in the main text). Bars indicate the mean number of averted hospitalizations in the high (A) and low (B) severity seasons in adults ≥ 65 from 1000 different Latin hypercube parameter combinations; error bars are the 95th percentiles. (C) and (D) show the corresponding results expressed as a percentage relative to burden at baseline. Each panel shows a different combination of the delay in administration of additional HDAVs (0, 3, or 6 weeks), and reduction in overall vaccine coverage (0, 10, or 20%). Positive values indicate a decrease in burden relative to the corresponding baseline simulation and therefore a positive impact of the new recommendation.



eFigure 10 – The reduction in overall vaccine coverage is most influential for overall outcomes. Partial rank correlation coefficient analyses assessing the impact of key parameters on the number of hospitalizations averted in adults ≥ 65 . Parameter ranges are given in eTable 1.



eFigure 11 – Increasing HDAV uptake following a preferential recommendation has a marginal effect on the threshold at which impacts switch from positive to negative. The increase in HDAV uptake following a preferential recommendation is fixed at 10% (A) or 15% (B). In both panels 75% of vaccinees ≥ 65 receive a HDAV at baseline and the relative VE of HDAVs compared to SVs is 15%.



eFigure 12 – Averted hospitalizations in adults ≥ 65 under different sampling distributions for relative VE. Bars indicate the mean number of averted hospitalizations from 1000 different Latin hypercube parameter combinations; error bars are the 95th percentiles. Colours indicate season severity (high or low) and distribution assumption (uniform or logit-normal). Each panel shows a different combination of the delay in administration of additional HDAVs (0, 3, or 6 weeks), and reduction in overall vaccine coverage (0, 10, or 20%). Positive values indicate a decrease in burden relative to the corresponding baseline simulation and therefore a positive impact of the new recommendation.

References

1. J. Asher, M. Clay, and Durham D. Aspr-flumodels, 13 September 2021.
2. United States Census Bureau. Census data 2020, 23 February 2021.
3. K. Prem, K. van Zandvoort, P. Klepac, R. M. Eggo, N. G. Davies, A. R. Cook, and M. Jit. Projecting contact matrices in 177 geographical regions: An update and comparison with empirical data for the COVID-19 era. *PLoS Computational Biology*, 17(7):e1009098, 2021.
4. CDC. FluVaxView Interactive, 23 September 2021.
5. CDC. FluView Interactive: ILI and Viral Surveillance.
6. W. Punpanich and T. Chotpitayasunondh. A review on the clinical spectrum and natural history of human influenza. *Int J Infect Dis*, 16(10):e714–723, 2012.
7. M. I. Meltzer, M. Gambhir, C. Y. Atkins, and D. L. Swerdlow. Standardizing scenarios to assess the need to respond to an influenza pandemic. *Clin Infect Dis*, 60 Suppl 1:S1–8, 2015.
8. C. Paules and K. Subbarao. Influenza. *The Lancet*, 390(10095):697–708, 2017.
9. T. Suess, C. Remschmidt, S. B. Schink, B. Schweiger, A. Heider, J. Milde, A. Nitsche, K. Schroeder, J. Doellinger, C. Braun, W. Haas, G. Krause, and U. Buchholz. Comparison of shedding characteristics of seasonal influenza virus (sub)types and influenza a(h1n1)pdm09; germany, 2007-2011. *PLoS One*, 7(12):e51653, 2012.
10. F. Carrat, E. Vergu, N. M. Ferguson, M. Lemaitre, S. Cauchemez, S. Leach, and A. J. Valleron. Time lines of infection and disease in human influenza: a review of volunteer challenge studies. *Am J Epidemiol*, 167(7):775–785, 2008.
11. Nancy H. L. Leung, Cuiling Xu, Dennis K. M. Ip, and Benjamin J. Cowling. The fraction of influenza virus infections that are asymptomatic. a review and meta-analysis. *Epidemiology*, 26(6):862–872, 2015.
12. M. Biggerstaff, C. Reed, D. L. Swerdlow, M. Gambhir, S. Graitcer, L. Finelli, R. H. Borse, S. A. Rasmussen, M. I. Meltzer, and C. B. Bridges. Estimating the potential effects of a vaccine program against an emerging influenza pandemic—united states. *Clin Infect Dis*, 60 Suppl 1:S20–29, 2015.
13. C. Cohen, J. Kleynhans, J. Moyes, M. L. McMorrow, F. K. Treurnicht, O. Hellferscee, A. Mathunjwa, A. von Gottberg, N. Wolter, N. A. Martinson, K. Kahn, L. Lebina, K. Mothlaoleng, F. Wafawanaka, F. X. Gómez-Olivé, T. Mkhencele, A. Mathee, S. Piketh, B. Language, and S. Tempia. Asymptomatic transmission and high community burden of seasonal influenza in an urban and a rural community in south africa, 2017–18 (PHIRST): a population cohort study. *The Lancet Global Health*, 9(6):e863–e874, 2021.

14. M. Biggerstaff, S. Cauchemez, C. Reed, M. Gambhir, and L. Finelli. Estimates of the reproduction number for seasonal, pandemic, and zoonotic influenza: a systematic review of the literature. *BMC Infect Dis*, 14:480, 2014.
15. CDC. Past Seasons Estimated Influenza Disease Burden, 28 September 2021.
16. CDC. Past seasons vaccine effectiveness estimates, 27 September 2021.
17. J. K. H. Lee, G. K. L. Lam, T. Shin, S. I. Samson, D. P. Greenberg, and A. Chit. Efficacy and effectiveness of high-dose influenza vaccine in older adults by circulating strain and antigenic match: An updated systematic review and meta-analysis. *Vaccine*, 39 Suppl 1:A24–A35, 2021.
18. H. S. Izurieta, Y. Chillarige, J. Kelman, Y. Wei, Y. Lu, W. Xu, M. Lu, D. Pratt, S. Chu, M. Wernecke, T. MaCurdy, and R. Forshee. Relative effectiveness of cell-cultured and egg-based influenza vaccines among elderly persons in the united states, 2017-2018. *J Infect Dis*, 220(8):1255–1264, 2019.
19. H. S. Izurieta, Y. Chillarige, J. Kelman, Y. Wei, Y. Lu, W. Xu, M. Lu, D. Pratt, M. Wernecke, T. MaCurdy, and R. Forshee. Relative effectiveness of influenza vaccines among the united states elderly, 2018-2019. *J Infect Dis*, 222(2):278–287, 2020.
20. H. S. Izurieta, M. Lu, J. Kelman, Y. Lu, A. Lindaas, J. Loc, D. Pratt, Y. Wei, Y. Chillarige, M. Wernecke, T. E. MaCurdy, and R. Forshee. Comparative effectiveness of influenza vaccines among u.s. medicare beneficiaries ages 65 years and older during the 2019-20 season. *Clin Infect Dis*, 2020.